molecules

MDPI

Article

Degradation of Benzotriazole UV Stabilizers in PAA/d-Electron Metal Ions Systems—Removal Kinetics, Products and Mechanism Evaluation

Dariusz Kiejza [1], Joanna Karpińska [2] and Urszula Kotowska [2,*]

[1] Doctoral School of Exact and Natural Sciences, University of Bialystok, Ciołkowskiego 1K St., 15-245 Białystok, Poland; d.kiejza@uwb.edu.pl
[2] Department of Analytical and Inorganic Chemistry, Faculty of Chemistry, University of Bialystok, Ciołkowskiego 1K St., 15-245 Białystok, Poland; joasia@uwb.edu.pl
* Correspondence: ukrajew@uwb.edu.pl; Tel.: +48-85-738-8111

Abstract: Benzotriazole UV stabilizers (BUVs) have gained popularity, due to their absorption properties in the near UV range (200–400 nm). They are used in the technology for manufacturing plastics, protective coatings, and cosmetics, to protect against the destructive influence of UV radiation. These compounds are highly resistant to biological and chemical degradation. As a result of insufficient treatment by sewage treatment plants, they accumulate in the environment and in the tissues of living organisms. BUVs have adverse effects on living organisms. This work presents the use of peracetic acid in combination with d-electron metal ions (Fe^{2+}, Co^{2+}), for the chemical oxidation of five UV filters from the benzotriazole group: 2-(2-hydroxy-5-methylphenyl)benzotriazole (UV-P), 2-tert-butyl-6-(5-chloro-2H-benzotriazol-2-yl)-4-methylphenol (UV-326), 2,4-di-tert-butyl-6-(5-chloro-2H-benzotriazol-2-yl)phenol (UV-327), 2-(2H-benzotriazol-2-yl)-4,6-di-tert-pentylphenol (UV-328), and 2-(2H-benzotriazol-2-yl)-4-(1,1,3,3-tetramethylbutyl)phenol (UV-329). The oxidation procedure has been optimized based on the design of experiments (DoE) methodology. The oxidation of benzotriazoles follows first order kinetics. The oxidation products of each benzotriazole were investigated, and the oxidation mechanisms of the tested compounds were proposed.

Keywords: benzotriazole UV stabilizers; peracetic acid; advanced oxidation processes; iron ions; cobalt ions

Citation: Kiejza, D.; Karpińska, J.; Kotowska, U. Degradation of Benzotriazole UV Stabilizers in PAA/d-Electron Metal Ions Systems—Removal Kinetics, Products and Mechanism Evaluation. *Molecules* **2022**, *27*, 3349. https://doi.org/10.3390/molecules27103349

Academic Editors: Dominique Agustin and Jana Pisk

Received: 1 May 2022
Accepted: 21 May 2022
Published: 23 May 2022

1. Introduction

UV stabilizers are, widely, used to prevent the degradation of polymeric products. UV radiation has a destructive effect on the structure of plastics, by changing the mass, color, gloss, and other properties, leading to a constant demand for compounds protecting them against UV degradation. As a result of their massive production, the global UV absorbers market is expected to reach a value of USD 669 million in 2020 and USD ~920 million by 2027 [1]. Benzotriazoles (BTRs) constitute a vast group of heterocyclic chemicals, including those with anti-corrosive and anti-icing properties as well as UV stabilizers (BUVs). The last group of BTRs are compounds containing an additional phenolic ring attached to the benzotriazole molecule (Figure 1).

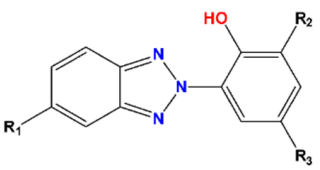

Figure 1. Benzotriazole UV stabilizer.

BUVs are used in the following products and fields: adhesives, engineering thermoplastics (UV-P), engineering plastics, sealants, wood lacquers (UV-326), coatings, fibers, films, lacquers (UV-327), automotive and industrial coatings, carpets, enamels, packaging, paints, photographic coating, plastics, stain, textiles, thermosetting acrylic enamels (UV-328), gel coats, glazing materials, marine and auto applications, molded articles, photoproducts, sheets, and signs (UV-329) [2]. The practical use of benzotriazoles dates back to the early 1960s, when the first patent for the use of benzotriazoles, as stabilizers for polymer products, was obtained [3]. BUVs are capable of absorbing UV light (300–400 nm) [4], and their protective properties have, also, used the production of cosmetics [5,6]. Benzotriazoles are expected to dominate the market for UV filters, due to their excellent spectral coverage and high molar extinction coefficient [1]. According to the OECD Existing Chemicals Database, UV-P, UV-328, and UV-329 are designated as high production volume chemicals (HPVC), with production >1000 tons per year [7]. Based on the SPIN database (Substances In Preparations In Nordic Countries), the total use of BUVs in Denmark, Finland, Norway, and Sweden are 0.4–11.6, 4–10, 0.1–0.9, 0.1–4.5, and 0.6 t/a for UV-P, UV-326, UV-327, UV-328, and UV-329, respectively [8].

Benzotriazoles are a serious environmental threat, due to their high resistance to both biological and chemical degradation. BUVs end up in the environment, as a result of direct rain runoff and snowmelt [9]; however, the largest contamination source is run-off from sewage treatment plants [10–16]. Due to their resistance to the degradation processes, benzotriazole-based UV absorbers accumulate and persist in the environment. The presence of benzotriazoles in aquatic environment, such as marine organisms, river and lake waters, and sediments, is a major threat [17–23]. In addition, UV-P, UV-326, UV-327, and UV-328 were detected in house dust [24,25]. BUVs were also determined in PM10 outdoor air, from industrial areas in Tarragona, Spain [26]. Benzotriazoles trends to accumulate in the tissues of living organisms [22,27–31] and were detected in human breast milk [32–34]. Exposure to benzotriazoles via food packaging seems insignificant but is, potentially, harmful. Dietary exposure to benzotriazoles, based on maximum concentrations in foods (ng/kg bw/day), are 9.5–29.7 and 38.7–120.4 for UV-326 and UV-329, respectively [35]. The concentrations of BUVs in various samples are presented in Table 1.

Table 1. Concentration of target benzotriazoles in environmental and biological samples.

Sample	Location	UV–P	UV–326	UV–327	UV–328	UV–329	Determination Method	Ref.
Breast milk (ng/g lipid wt.)	South Korea	19.2	1.77	10	64.3	4.54	GC-MS	[32]
	Japan	21	0.08	n.d.	0.2	3.8	UHPLC-MS/MS	[33]
	Philippines	16/71 [a]	34/64	n.d.	2.4/1.9	n.d.		
	Vietnam	91/3.9/32	0.53/n.d./2.1	n.d./n.d./1.6	0.9/0.48/0.47	9.6/2.6/6		
Mussels (ng/g)	Asia-Pacific coastal waters	–	150	68	130	–	GC-MS	[36]
WWTP (ng/L)	China	9.9–37.1 (7.2–15.9) [b]	–	–	2.6–2.9 (0.60)	3.8	LC-MS/MS	[16]
Rivers in India (ng/L)	Water	0.2–2.3	1.5–3.7	3.3–4.3	0.5–3.4	8.1–13.7	GC-MS	[21]
	Sediment	0.1–0.3	0.2–0.5	0.6–2	0.2–0.9	0.9–1.41		
	Fish	2.2–6.9	0.6–1.6	1.0–3.2	0.2–1.6	3.0–7.4		
House dust (ng/L)	Philippines	–	53/6.2	28/10	50/18	–	UHPLC-ESI-MS/MS	[24]
Blood plasma of water animals (pg/g)	North America	–	–	–	240–776	<640	UPLC-MS/MS	[22]

[a]—the concentration after the slash applies to different locations; [b]—concentration in influent (effluent).

Benzotriazoles raise concerns about the safety of living organisms and their surrounding environment. Only two of the benzotriazoles studied in this work are regulated by law. The European Chemicals Agency (ECHA) has classified UV-327 and UV-328 as substances with high bioaccumulation potential and strong resistance to degradation. UV-327 is on the list of substances considered as persistent organic pollutants (POPs). The Japanese government, also, classified UV-327 as a Monitoring Chemical Substance because of its

high bioaccumulative characteristics [37]. The 16th meeting of the Persistent Organic Pollutants Review Committee of the Stockholm Convention (January 2021) concluded that UV-328 satisfies all the criteria to be included in the convention's Annex D (Screening criteria for persistent organic pollutants), namely due to is persistence, bioaccumulation, potential for long-range environmental transport, and adverse effects on humans and/or the environment [38].

All benzotriazoles presented in this study raise doubts about their safety because they may contribute to adverse antiandrogenic effects [39]. Feng et al. [40] has proven that UV-P shows partial estrogenic activity against the human breast cancer MVLN cell line, while UV-329 is not estrogenic. In vitro experiments with human liver microsomes (HLMs) were performed, to identify the phase I metabolites of UV-327 and UV-328, which can be used as potential biomarkers for exposure to these compounds [41,42]. UV-328 metabolites are, also, detected in human urine and blood [43,44]. Detection of metabolites can elucidate the pathway of metabolism and estimate the toxicity of specific metabolism products towards living organisms. The UV-328 and UV-P metabolites have greater antiandrogenic activity upon human CYP3A4-mediated biotransformation than their non-metabolized forms [45]. UV-328, adversely, affects the thyroid hormone pathway of the zebrafish, Danio rerio [46]. Chronic exposure to low concentrations of this UV stabilizer causes oxidative stress and liver damage in zebrafish [47]. Freshwater green algae *Chlamydomonas reinhardtii* subjected to UV-328 show increased production of reactive oxygen species, while prolonged contact with UV-234 caused an increase in lipid peroxidation [48]. Knowledge about concentrations that cause negative effects on living organisms is limited, with only a few studies available for the toxicity assessment of BUVs (Table 2.).

Table 2. Acute toxicity of selected benzotriazoles on living organisms.

BUVs	Route	Living Organism	Acute Toxicity LD_{50}/LC_{50}	Ref.
UV-P	oral	Freshwater crustacean (*Daphnia pulex*)	>10 mg/L	[49]
	oral	mice	>5–>10 g/kg	[50]
	oral	rats	>15 g/kg	
	oral	rats	>5 g/kg	
	inhalation	rats	1420 mg/m^3	
	dermal	rabbits	>2 g/kg	
	dermal	Guinea pigs	>3 g/kg	
UV-328	oral	Rat	7750 mg/kg	[51]
	inhalation	Rat	400 mg/m^3	
	dermal	rabbit	1100 mg/kg	
	direct	Algae *Raphidocelis subcapitata*	EC_{50} > 0.016 mg/L	[52]

The aim of the presented work was to develop a new approach to the removal of BUVs as persistent environmental pollutants from aqueous solutions, based on the use of advanced oxidation. The literature review shows that, until now, no attempt has been made to use chemical oxidants to degrade and dispose of BUVs. This work presents the study on the oxidation process of five benzotriazole UV stabilizers that use peracetic acid activated with d-electron metal ions. Peracetic acid (PAA) is a long-known disinfectant and effective oxidant of organic micropollutants [53–56]. In recent studies, UV irradiation [57–60], d-electron metal ions [61–64], or heterogeneous activators [65–71] have been used as PAA activators. So far, no information is available on the removal procedures of benzotriazole UV stabilizers. Liu et al. [72] reported that sorption on sludge plays a dominant role in the removal of benzotriazole UV absorbers in municipal wastewater treatment plants. Chen et al. [73] described the photodegradation process of UV-P in coastal seawaters. The neutral form of UV-P is photodegraded more slowly than both the cationic and the anionic form. Singlet oxygen, hydroxyl radical, and dissolved organic matter have a positive effect on indirect UV-P photodegradation, in coastal seawaters. One of the latest reports appeared

on the reductive photodegradation of BUVs in visible light, using tetraacetylated riboflavin (RFTA) as a photocatalyst [74].

2. Results and Discussion

2.1. Optimization of the UV Stabilizers Oxidation Process

Twenty experiments, including six repetitions under the same conditions in the central point, were carried out for three selected factors that affect oxidation efficiency at five levels. Table 3, Tables S2 and S3 present data for the individual experiments as well as for the experimental and predicted values of removal efficiency (RE%).

Table 3. The three-factor CCD matrix, with the experimental and predicted removal efficiency values for UV-326 degradation.

	$[PAA]_0$ (mg/L)	$[Me^{2+}]_0$ (mol/L)	PAA/Fe^{2+} System			PAA/Co^{2+} System		
			pH	RE% (exp.)	RE% (pred.)	pH	RE% (exp.)	RE% (pred.)
1	45	3.45×10^{-4}	4.6	91.01	100.00	7	57.35	63.37
2	45	3.45×10^{-4}	3.4	94.13	97.24	4	76.25	77.84
3	45	1.45×10^{-5}	4.6	36.99	55.25	7	73.69	72.96
4	45	1.45×10^{-5}	3.4	33.35	46.27	4	55.32	60.78
5	15	3.45×10^{-4}	4.6	97.44	100.00	7	66.91	64.61
6	15	3.45×10^{-4}	3.4	92.99	97.24	4	75.48	79.08
7	15	1.45×10^{-5}	4.6	20.10	55.25	7	75.22	74.20
8	15	1.45×10^{-5}	3.4	23.84	46.27	4	49.54	62.02
9	55	7×10^{-5}	4	78.68	66.76	5.5	67.55	66.21
10	5	7×10^{-5}	4	93.51	66.76	5.5	65.49	68.28
11	30	1×10^{-3}	4	90.15	87.04	5.5	65.51	64.61
12	30	5×10^{-6}	4	41.04	53.29	5.5	55.44	66.56
13	30	7×10^{-5}	5	93.50	61.48	8	64.78	76.62
14	30	7×10^{-5}	3	57.71	46.51	3	58.76	63.78
15	30	7×10^{-5}	4	75.96	66.76	5.5	69.46	67.68
16	30	7×10^{-5}	4	76.79	66.76	5.5	77.01	67.68
17	30	7×10^{-5}	4	71.59	66.76	5.5	77.37	67.68
18	30	7×10^{-5}	4	72.02	66.76	5.5	77.74	67.68
19	30	7×10^{-5}	4	72.57	66.76	5.5	81.38	67.68
20	30	7×10^{-5}	4	78.93	66.76	5.5	76.76	67.68

exp.—experimental; pred.—predicted.

For each of the studied UV stabilizers (UV-P, UV-326, UV-327, UV-328, UV-329), a mathematical model was developed to characterize the relationship between the degradation efficiency, PAA, metal ion concentration, and pH of the solution. Statistical analysis of the developed regression model was performed for all benzotriazoles. ANOVA test results for fit UV-326 removal efficiency are presented in Table 4. Data for other benzotriazoles are included in the Supplementary Materials (Tables S4–S10).

Table 4. ANOVA results for UV-326 removal efficiency from CCD.

Source of Variation	Sum of Squares	DF	Mean Square	*F*-Value	*p*-Value
PAA concentration (square)	128.572	1	128.5723	8.46121	0.033446
Co^{2+} concentration (linear)	103.937	1	103.9369	6.83998	0.047364
Co^{2+} concentration (square)	165.885	1	165.8846	10.91670	0.021380
pH (square)	308.624	1	308.6242	20.31025	0.006360
Co^{2+} concentration-pH interactions	585.017	1	585.0169	38.49937	0.001588
Lack of fit	507.354	9	56.3727		
Pure error	75.977	5	15.1955		
Total	1610.347	19			
R^2 = 0.63776	R^2 (adjusted) = 0.50839		$p < 0.05$ is considered as significant		

The results obtained for UV-326 indicate that the regression model is characterized by a low coefficient of determination (R^2 = 0.638). These results prove that the model only determines the influence of factors on the effectiveness of UV-326 removal in 64%.

Pareto charts (Figure 2, Figures S5 and S6) show a statistically significant ($p < 0.05$) influence of the individual independent variables on the UV stabilizers removal process. The presented diagrams show that the efficiency of micropollutants removal, most strongly, depends on the concentration of metal ions. In addition, the relationship between the concentration of the metal ion and the pH is noticeable because it determines the speciation of the activator necessary for the oxidation process initiation. In the Co^{2+}/PAA process, all factors have a statistically insignificant effect on the removal efficiency of UV-327 and UV-328. This gives the information that any amount of oxidant and activator is good for these substances' removal.

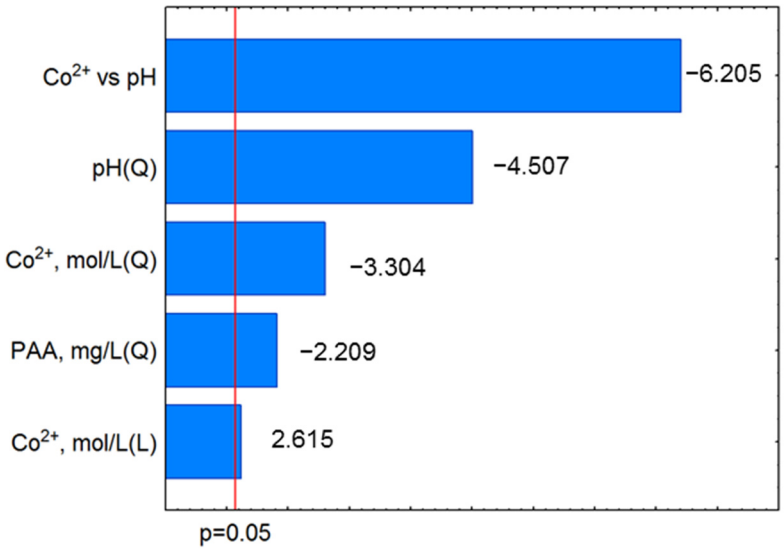

Figure 2. Absolute values of the standardized effects of UV-326 degradation in Co^{2+}/PAA process.

Figure 3, Figures S7 and S8 present response surface plots of the removal efficiency of UV stabilizers depending on the combination of two independent variables: PAA concentration vs. pH, PAA concentration vs. metal ion concentration, and metal ion concentration vs. pH, with a predetermined value of the third variable. As can be seen in the graphs, there is no agreement as to the influence of a specific factor on the oxidation of benzotriazoles; however, a strong dependence of RE% on the concentration of PAA and the activator is observed. The higher the concentration of the oxidant and/or activator is, the greater the percent of degradation. This phenomenon can be explained by the fact that the number of radicals generated increases with an increase in PAA concentration. After exceeding the optimal concentration values, the oxidation efficiency may drop. It is observed that in the Fe^{2+}/PAA process, the excess of PAA may interact with hydroxyl radicals, leading to the formation of radicals with lower reactivity [75]:

$$CH_3C(O)O_2H + {}^{\bullet}OH \rightarrow CH_3C(O)O_2{}^{\bullet} + CH_3C(O)OH \quad (1)$$

$$CH_3C(O)O_2H + {}^{\bullet}OH \rightarrow CH_3C(O)^{\bullet} + H_2O + O_2 \quad (2)$$

$$CH_3C(O)O_2H + {}^{\bullet}OH \rightarrow HO_2{}^{\bullet} + CH_3C(O)OH \quad (3)$$

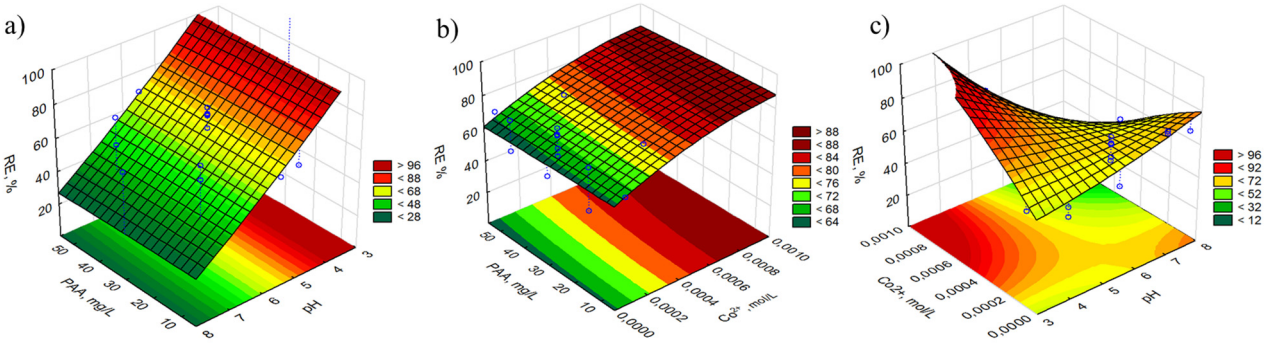

Figure 3. Response surface plots of RE%, as the function of two independent variables: (**a**) C_{PAA} and pH, (**b**) C_{PAA} and C_{Co2+}, and (**c**) C_{Co2+} and pH. Conditions: $[PAA]_0 = 40$ mg/L, $[Co^{2+}]_0 = 8 \times 10^{-4}$ mol/L, pH = 4.5.

There may be a situation where the excess PAA can react with acetoxyl radicals, resulting in the formation of less-reactive acetylperoxyl radicals:

$$CH_3C(O)O_2H + CH_3C(O)O^{\bullet} \rightarrow CH_3C(O)O_2^{\bullet} + CH_3C(O)OH \quad (4)$$

For UV-327 and UV-328 in the Co^{2+}/PAA process, no factor significantly contributes to the degradation efficiency. Various combinations of the independent variables result in the same oxidation value, of about 70%. It led to the conclusion that with any amount of oxidant and/or activator, and at any pH, it is possible to carry out the oxidation process. In both processes, the pH contributes to the efficiency of the UV stabilizer removal process. The pH of the system affects the radical formation process as well as the chemical forms of the oxidant and activators. Kim et al. [75] reported that PAA (pKa 8.2) at a pH of 3–7 exists in the form of neutral molecules. With increasing pH, the concentration of the ionized form increases. PAA^- shows weaker oxidizing properties than PAA^0, but can react more easily with $^{\bullet}OH$ radicals, thus affecting the oxidation process. At a higher pH, Fe^{2+} can be oxidized more easily. Moreover, Fe^{3+} speciation is strongly dependent on pH; hydroxocomplexes may form or they may precipitate. The precipitated forms of iron are unable to activate the peracid which, in turn, reduces the concentration of radicals in the system.

Mechanisms of peracetic acid-based advanced oxidation processes are not, yet, well understood. The radicals formed as a result of PAA activation are not highly reactive but can be selective; therefore, optimization of the oxidation process brings different results for individually tested organic micropollutants. Nevertheless, optimization allows one to predict the success of the removal process. On the basis of the obtained results, it was found that the optimal conditions for the oxidation of UV stabilizers were $C_{PAA} = 25$ mg/L and $C_{Fe2+} = 6{\cdot}10^{-4}$ mol/L for the Fe^{2+}/PAA process, and $C_{PAA} = 40$ mg/L and $C_{Co2+} = 8 \times 10^{-4}$ mol/L for the Co^{2+}/PAA process. Both experiments were performed at a pH of 4.5.

2.2. UV Stabilizers Degradation Kinetics

Degradation of UV-P, UV-326, UV-327, UV-328, and UV-329 was investigated, at a pH of 4.5, in the Fe^{2+}/PAA and Co^{2+}/PAA systems. Initial benzotriazoles concentrations were 500 µg/L. In the Fe^{2+}/PAA system, $[Fe^{2+}]_0 = 6 \times 10^{-4}$ mol/L and $[PAA]_0 = 25$ mg/L, while in Co^{2+}/PAA, $[Co^{2+}]_0 = 8 \times 10^{-4}$ mol/L and $[PAA]_0 = 40$ mg/L. In the Fe^{2+}/PAA process, 69%, 90%, 91%, 91%, and 89% degradation in 180 min was observed for UV-P, UV-326, UV-327, UV-328, and UV-329, respectively. UV-P is the least oxidized among all tested compounds. Similar results were obtained in the Co^{2+}/PAA process, for the same time frame (180 min), where 96%, 95%, 91%, 89%, and 80% of UV-P, UV-326, UV-327, UV-328, and UV-329, respectively, were oxidized. In the case of UV-P, an immediate decrease in concentration was noticed within 5 min. This time is too short for the oxidation of the mentioned compound, since UV stabilizers are relatively difficult to degrade. This result

can, potentially, be explained in two ways. In the Co^{2+}/PAA system, either selective oxidation of UV-P takes place with only subsequent compounds created, or there is no oxidation process, with only the UV-P complexation reaction by cobalt ions [2,76]. The kinetics of tested compounds decomposition are presented in Figures 4 and 5.

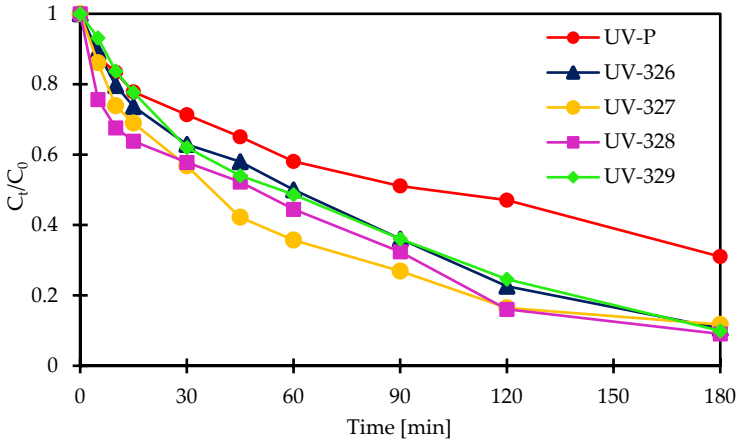

Figure 4. Kinetics of BUVs's degradation in Fe^{2+}/PAA process. Reaction conditions: $[PAA]_0$ = 25 mg/L, $[Fe^{2+}]_0 = 6 \times 10^{-4}$ mol/L, initial pH 4.5.

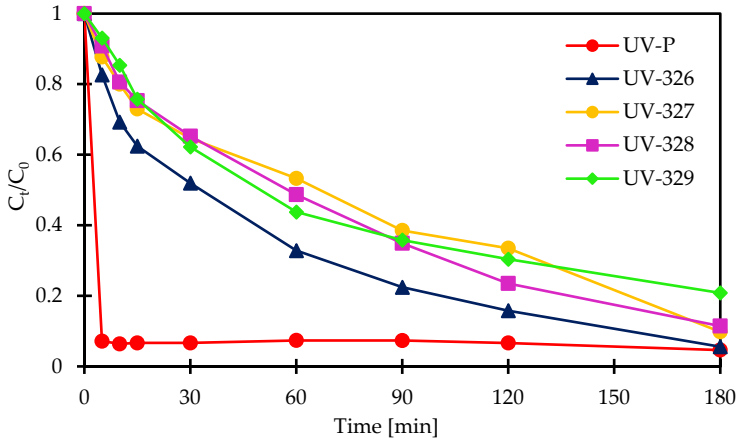

Figure 5. Kinetics of BUVs's degradation in Co^{2+}/PAA process. Reaction conditions: $[PAA]_0$ = 40 mg/L, $[Co^{2+}]_0 = 8 \times 10^{-4}$ mol/L, initial pH 4.5.

Pseudo-first order kinetic model was applied to determin the rate of tested organic micropollutants. First-order kinetic constants in the Fe^{2+}/PAA process were 0.0059 min^{-1}, 0.0118 min^{-1}, 0.0166 min^{-1}, 0.0125 min^{-1}, and 0.0121 min^{-1}, for UV-P, UV-326, UV-327, UV-328, and UV-329, respectively. Similar values were obtained in the Co^{2+}/PAA process, where *k* was 0.0150 min^{-1}, 0.0107 min^{-1}, 0.0116 min^{-1}, and 0.0088 min^{-1} for UV-326, UV-327, UV-328, and UV-329, respectively (Table 5).

Table 5. Determination coefficients (R^2), first-order constant (k), and half-life time ($t_{1/2}$), of BUVs's removal by Fe^{2+}, for Co^{2+}/PAA-based oxidation.

Compound	Fe^{2+}/PAA Process			Co^{2+}/PAA Process		
	R^2	k (min^{-1})	$t_{1/2}$ (min)	R^2	k (min^{-1})	$t_{1/2}$ (min)
UV-P	0.972	0.0059	117.48	–	–	–
UV-326	0.992	0.0118	58.74	0.992	0.0150	46.21
UV-327	0.967	0.0166	41.76	0.953	0.0107	64.78
UV-328	0.976	0.0125	55.45	0.997	0.0116	59.75
UV-329	0.991	0.0121	57.28	0.960	0.0088	78.77

2.3. Mechanism of UV Stabilizers Degradation

Commercial peracetic acid is, typically, an equilibrated mixture of PAA, hydrogen peroxide, acetic acid, and water, according to the reaction:

$$CH_3CO_2H + H_2O_2 \leftrightarrow CH_3C(O)O_2H + H_2O \quad (5)$$

For this reason, activation of peracetic leads to the generation of reactive species involved in the oxidation of organic micropollutants. Using homogenous systems, such as UV irradiation andd-electron metal ions, $^{\bullet}OH$, $CH_3C(O)OO^{\bullet}$, $CH_3C(O)O^{\bullet}$, and other radicals can be formed [57,58,61,62,75]. In the Fe^{2+}/PAA process, Fe^{2+} reacts with PAA and H_2O_2. The reactions that take place are as follows [75]:

$$CH_3C(O)OOH + Fe^{2+} \rightarrow CH_3C(O)O^{\bullet} + Fe^{3+} + OH^- \quad (6)$$

$$CH_3C(O)OOH + Fe^{2+} \rightarrow CH_3C(O)O\text{-} + Fe^{3+} + {}^{\bullet}OH \quad (7)$$

$$CH_3C(O)OOH + Fe^{2+} \rightarrow CH_3C(O)OH + Fe^{IV}O^{2+} \quad (8)$$

$$H_2O_2 + Fe^{2+} \rightarrow {}^{\bullet}OH + Fe^{3+} + OH^- \quad (9)$$

$$H_2O_2 + Fe^{2+} \rightarrow H_2O + Fe^{IV}O^{2+} \quad (10)$$

The main reactions taking place within the Co^{2+}/PAA system are the formation of acetylperoxy ($CH_3C(O)OO^{\bullet}$) and acetoxyl ($CH_3C(O)O^{\bullet}$) from both cobalt species [61,62]:

$$CH_3C(O)OOH + Co^{2+} \rightarrow CH_3C(O)O^{\bullet} + Co^{3+} + OH^- \quad (11)$$

$$CH_3C(O)OOH + Co^{3+} \rightarrow CH_3C(O)OO^{\bullet} + Co^{2+} + H^+ \quad (12)$$

The mechanisms of the Fe^{2+}/PAA and Co^{2+}/PAA processes have been investigated, by determining the participation of individual radicals in the oxidation process of UV-stabilizers. To evaluate the $^{\bullet}OH$ radicals' activity, tert-butyl alcohol (TBA) was used. The participation of $O_2^{\bullet-}$ radical and $^1O_2$ was also checked, by adding 1,4-BQ and NaN_3 to the solution for superoxide anion radical and singlet oxygen, respectively. The influence of individual reactive species, on the removal efficiency of tested UV stabilizers in the Fe^{2+}/PAA and Co^{2+}/PAA systems, is shown in Figures 6 and 7.

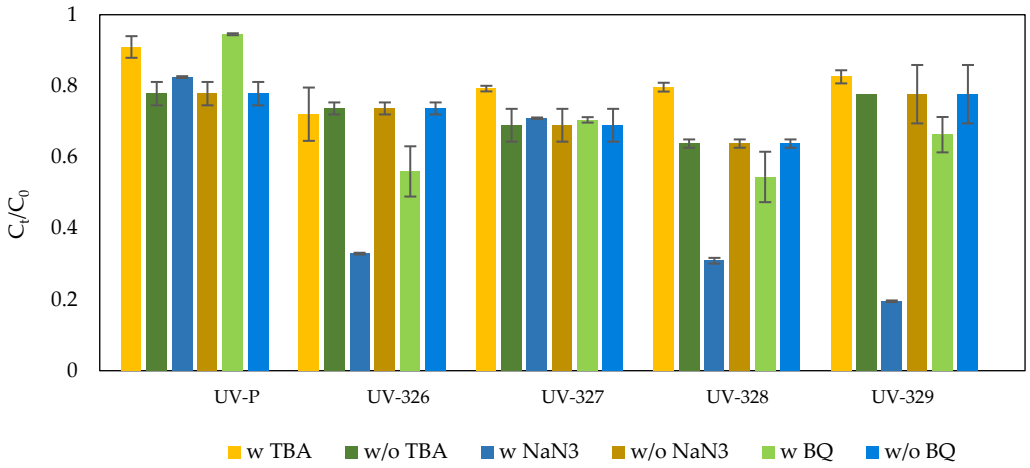

Figure 6. Effect of radical scavengers on UV stabilizers' degradation in the Fe^{2+}/PAA process (w"—reaction with radical quencher, w/o"—reaction without radical quencher).

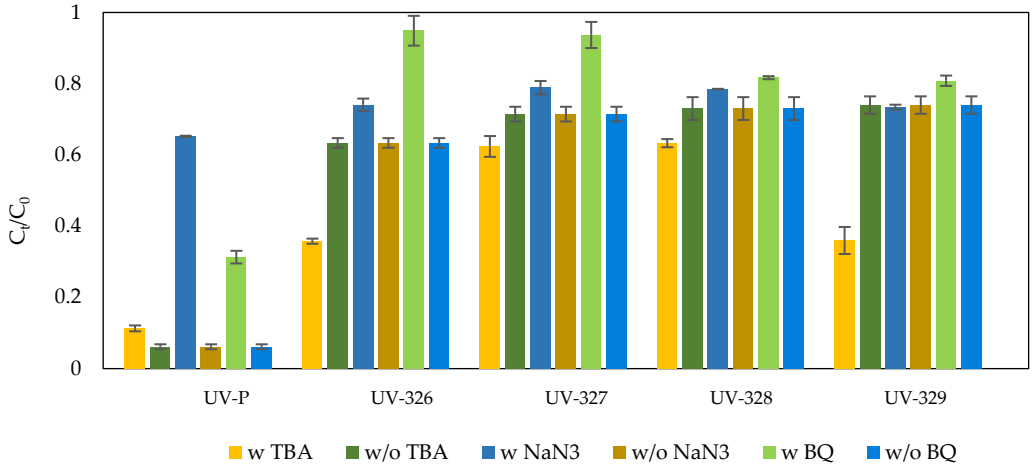

Figure 7. Effect of radical scavengers on UV stabilizers' degradation in the Co^{2+}/PAA process (w"—reaction with radical quencher, w/o"—reaction without radical quencher).

There are two main sources of hydroxyl radicals in the Fe^{2+}/PAA process. $^{\bullet}OH$ radicals are formed from the direct reaction of PAA with iron ions and from the Fenton reaction taking place in the system, due to the presence of H_2O_2. The much higher reaction rate constant for the formation of radicals from peracetic acid at pH of 3.0–7.1 (0.5–1.10) × 10^5 $M^{-1}{\cdot}s^{-1}$, compared to that of Fe^{2+}/H_2O_2 (k = 63–76 $M^{-1}{\cdot}s^{-1}$), proves that PAA decomposition is the predominant source of $^{\bullet}OH$ radicals in Fe (II)/PAA systems [54]. As seen in Figure 1, the oxidation process of benzotriazoles takes place with a small share of hydroxyl radicals. Sodium azide, used as $^1O_2$ quencher, increased the removal efficiency for almost all benzotriazoles. This phenomenon can be explained by the fact that at pH of 4–13, the N_3^- ion can react with hydroxyl radicals to form azide radicals $N_3^{\bullet}$, which, in turn, could oxidize organic compounds by electron transfer [77]:

$$^{\bullet}OH + N_3 \rightarrow OH^- + N_3^{\bullet} \quad (13)$$

In the Co^{2+}/PAA process, this phenomenon is not observed because fewer $^{\bullet}OH$ radicals that can oxidize azide are produced. This result may, indirectly, prove the presence of hydroxyl radicals in the iron (II)-activated PAA system. Superoxide anion radicals can, also, be formed in the system, as a result of the reaction accompanying the Fenton process:

$$H_2O_2 + {}^{\bullet}OH \rightarrow HO_2^{\bullet} + H_2O \quad (14)$$

$$HO_2^{\bullet} \rightarrow O_2^{\bullet -} + H^+ \quad (15)$$

$O_2^{\bullet -}$ may react with $CH_3C(O)OO^{\bullet}$ [62], which removes radicals affecting the degradation process of UV stabilizers:

$$CH_3C(O)OO^{\bullet} + O_2^{\bullet -} \rightarrow CH_3C(O)OO^- + O_2 \quad (16)$$

The removal of superoxide anion, with 1,4-BQ from the system, increased the removal efficiency of most benzotriazoles. The use of tert-butyl alcohol does not cause any significant changes in the efficiency of benzotriazole removal, which proves the low participation of hydroxyl radicals in the Co^{2+}/PAA process. $^{\bullet}OH$ are not generated in the direct reaction of PAA with Co^{2+} ions, although these can be formed from R-$O^{\bullet}$ radicals [62]. Singlet oxygen is produced by the decomposition of PAA [62,78]:

$$CH_3C(O)OOH + CH_3C(O)OO^{-(} \rightarrow CH_3CH(O)OH + CH_3C(O)O^{-(} + {}^1O_2 \quad (17)$$

The effectiveness of BTA removal under the influence of singlet oxygen was assessed, by adding NaN_3 to the reaction mixture. Sodium azide did not contribute to the slowing

down of the UV stabilizers degradation process. It follows that singlet oxygen is formed in too small of an amount, which is not capable of efficient oxidation of organic micropollutants. $HO_2^{\bullet}/O_2^{\bullet-}$ radicals can be formed in the Co^{2+}/PAA process, both from other radicals and through a reaction with hydrogen peroxide [62,75]:

$$CH_3C(O)OO^{\bullet} \rightarrow HO_2^{\bullet} + CH_2CO \quad (18)$$

$$H_2O_2 + CH_3C(O)OO^{\bullet} \rightarrow HO_2^{\bullet} + CH_3C(O)OOH \quad (19)$$

$$CH_3C(O)O^{\bullet} + H_2O_2 \rightarrow HO_2^{\bullet} + CH_3C(O)OH \quad (20)$$

$$CH_3C(O)OO^{\bullet} + H_2O_2 \rightarrow HO_2^{\bullet} + CH_3C(O)OOH \quad (21)$$

As can be seen in the figure, superoxide anion has the greatest influence on the oxidation process of UV-326 and UV-327.

2.4. Benzotriazole UV Stabilizers Degradation Products

ESI-MS analysis of the oxidation products of the tested benzotriazoles was performed, and mass spectra were acquired (Figure S9). The registered spectra of post-reaction mixtures are similar because of the similar structures analyzed BUVs, therefore, some identical degradation products have been detected. On the other hand, the ions were characteristic, only for products made from only one of the benzotriazoles. Based on the ESI-MS spectra and the available literature data [79–81], the structures of the oxidation products have been proposed (Figure 8, Table S11). Most of the structural changes occur within the benzotriazole ring, which was discussed in previous works. When comparing the oxidation products in the Fe^{2+}/PAA and Co^{2+}/PAA processes, no significant differences were noticed. Some products contain -OH groups, resulting from the action of the hydroxyl radical. It confirms its dominant role in the oxidation process. Generally, products with lower molecular weights are produced. This shows that the radicals break the molecules into smaller fragments and, probably, lead to complete mineralization.

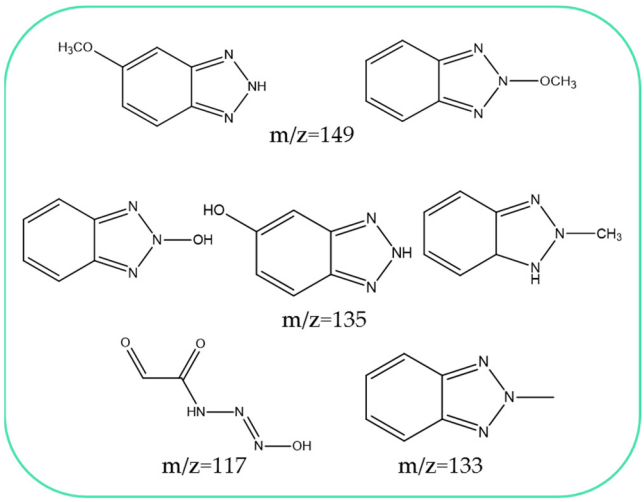

Figure 8. Proposed structures of benzotriazole UV stabilizers' oxidation products.

3. Materials and Methods

3.1. Materials and Characterizaton

Benzotriazole UV stabilizers: UV-P, UV-326, UV-327, UV-328, UV-329 were obtained from Sigma-Aldrich (Steinheim am Albuch, Germany). Characteristics of UV stabilizers considered within this work are included in Table S1 of the Supplementary Materials. All standard reagents were at analytical grade. These were used to prepare a stock solution that contained 1 mg/mL of each chemical in acetonitrile, that was then stored at −18 °C, for no longer than one month. Working solutions, prepared by diluting the stock

standard solution in acetonitrile, were stored at −18 °C, for no longer than two weeks. Chromatography-grade pure acetonitrile, supplied by Merck (Darmstadt, Germany), was used. Chromatography-grade pure chlorobenzene, produced by Sigma-Aldrich (Steinheim am Albuch, Germany), was applied as the extraction solvent. Ferrous sulfate heptahydrate ($FeSO_4 \cdot 7H_2O$) (Chempur, Piekary Śląskie, Poland) and cobalt sulfate ($CoSO_4$) (Sigma Aldrich, Steinheim am Albuch, Germany) were used to activate peracetic acid. Peracetic acid was synthesized on site, according to the procedure described in Supplementary Materials. For this purpose, pure p.a. acetic acid, hydrogen peroxide (Chempur, Piekary Śląskie, Poland), and sulphuric acid (POCH, Gliwice, Poland) were used. Sodium thiosulfate ($Na_2S_2O_3$), obtained from Thermo Fisher Scientific (Dreieich, Germany), was used as a radical scavenger. Tert-butyl alcohol TBA and sodium azide NaN_3, acquired from Fisher Scientific (Merelbeke, Belgium), and 1,4-benzoquinone 1,4-BQ (Acros Organics, Geel, Belgium) were used to study the reaction mechanisms. Deionized water from the Milli-Q RG (Millipore, Burlington, MA, USA) purification system was stored in glass bottles.

Determination of the UV stabilizers in water samples was performed by gas chromatography with mass spectrometry (GC-MS). The chromatographic analysis was carried out, using a 7890B gas chromatograph with an electronic pressure control, and was coupled with a mass selective detector 5977A (electron impact source and quadrupole analyzer) from Agilent Technologies, USA. This device was equipped with an HP-5MS column (5% phenylmethylsiloxane), with dimensions of 30 m × 0.25 mm × 0.25 µm film thickness. Helium (99.999%), at a constant flow rate of 1.0 mL/min, was used as a carrier gas. An injector worked in splitless mode, at a temperature of 250 °C. The oven was operating on the following temperature schedule: start at 120 °C, raise the temperature by increments of 10 °C/min, until reaching 290 °C, then, by increments of 20 °C, until reaching 310 °C. Each temperature was maintained for 1 min, for a total run time of 19 min. The electron impact source temperature was 230 °C, with electron energy of 70 eV. The quadrupole temperature was 150 °C, and the GC interface temperature was 280 °C. The MS detector was set to work in selected ion monitoring (SIM) mode. Target compound monitored ions are shown in Table S1 of the Supplementary Materials. Then, calibration curves were prepared to calculate BUVs's concentrations during the oxidation reaction (Figure S4).

In order to identify the oxidation products, analyses were performed using an Agilent 6530 Accurate-Mass Q-TOF ESI (+) and LC/MS system, equipped with an Agilent Poroshell 120 EC-C18 column (2.7 µm × 3.0 × 150 mm). The gradient mobile phase was A: water, B: methanol at flow rate 0.3 mL/min, for UV-P, UV-326, and UV-329: 0–5.50 min 20% A, 9.00 min 1% A, 15.00 min 1%, A 15.50 min 20% A, and 18.00 min 70% A; for UV-327 and UV-328: 0–5.50 min 20% A, 9.00 min 1% A, 15.00 min 1% A 15.50 min 20% A, 18.00 min 70% A, 24.00 min 20% A, 29.00 min 1% A, 35.00 min 1% A 35.50 min 20% A, and 38.00 min 70% A.

Optimization of the benzotriazole oxidation process was made in Statistica 13.1 software (Tibco Software Inc., Palo Alto, CA, USA), using the Central Composite Design (CCD) technique from the design of experiments (DoE) method.

3.2. Procedure of Ultrasound-Assisted Emulsification Microextraction

The efficiency of BUVs's extraction, using various organic solvents was tested. For this purpose, the ultrasound-assisted emulsification microextraction (USAEME) process was performed using chlorobenzene, chloroform, and toluene as extraction solvents. Additionally, USAEME, with solidification of the floating organic drop method (SFOD), using 1-undecanol and hexadecane, was used. Aliquots, of 5 mL of a water sample containing benzotriazoles, were placed in 10 mL glass centrifuge tubes. Then, 80 µL of extractant was added to the water sample and mixed. Immediately after, the tube was immersed in a Sonorex Digitec 102H ultrasonic water bath, Bandelin (Germany). Extractions were performed at 42 kHz of ultrasound frequency and 230 W of power, for 10 min at room temperature. The solvent volume of 80 µL and extraction time of 10 min were considered optimal, based on preliminary tests. Emulsions were disrupted by centrifugation, at 4000 rpm for 5 min, in an MPW-M UNIVERSAL Med. Instruments (Poland) laboratory

centrifuge. Then, the organic phase settled at the bottom of the conical tube. After centrifugation, the organic layer was collected, using a 100 µL Agilent Technologies (USA) syringe and transferred into a 150 µL microvial with integrated insert. Then, extracts were subjected to GC-MS analysis. Chromatogram and mass spectra of tested benzotriazoles are shown in Figures S1 and S2. Results obtained for UV stabilizers indicate that the optimal extraction solvent is chlorobenzene (Figure S3), and this extractant was, then, used in all subsequent experiments.

3.3. Degradation Experiments

The preliminary degradation experiments of benzotriazoles were carried out in glass beakers, by mixing certain volumes of metal ions and benzotriazoles mixture, with an initial concentration of 500 µg/L. The pH of the mixture was adjusted, by adding a few microliters of NaOH (0.5 mol/L). Then, an appropriate volume of peracetic acid working solution was added to initiate the reaction. The oxidation reaction was carried out for 30 min, with continuous stirring of the solution at 700 rpm. Then, 800 µL 20% sodium thiosulfate was added, to stop the reaction. Quenching experiments were conducted by adding 0.5 mol/L TBA, 0.1 mol/L NaN_3, or 0.01 mol/L 1,4-BQ into reaction solutions, before initiating a reaction. The experiment was carried out in dark conditions, to prevent the PAA from being activated by light.

4. Conclusions

For the first time, a procedure for advanced oxidation of benzotriazole UV filters, using peracetic acid activated with d-electron metal ions, was developed. A CCD-based chemometric approach was used to optimize of the oxidation process. At pH = 4.5, $[PAA]_0$ = 25 mg/L and $[Fe^{2+}]_0 = 6 \times 10^{-4}$ mol/L as well as $[PAA]_0$ = 40 mg/L and $[Co^{2+}]_0 = 6 \times 10^{-4}$ mol/L, the best oxidation efficiency of benzotriazoles was achieved. The effectiveness of the oxidizing system depends on the ratio of the concentration of peracetic acid and the activator, and, also, on the type of oxidized compound. Nevertheless, a slight advantage of the Fe^{2+}/PAA system, over the system containing Co^{2+} ions as the PAA activator, is noticeable. Iron ions generate more reactive hydroxyl radicals and, therefore, increase the rate and efficiency of the oxidation reaction. Conducting experiments with the use of TBA, NaN_3, and 1,4-BQ confirmed the earlier reports on the dominant role of $^{\bullet}OH$ radicals in the Fe^{2+}/PAA process, and the influence of $CH_3C(O)OO^{\bullet}$ and $CH_3C(O)O^{\bullet}$ radicals on the oxidative activity of the Co^{2+}/PAA system. This work extends the existing knowledge on the use of chemical oxidants to remove persistent pollutants from water matrices. The conducted research contributes significantly to the research on the oxidation processes in peracetic acid/d-electron metal ions systems, as the literature to date concerns only a few compounds exposed to these systems.

Supplementary Materials: The following supporting information can be downloaded at: https://www.mdpi.com/article/10.3390/molecules27103349/s1, Table S1: the chemical structure, chemical abstract service (CAS) registry number, molecular weights (MW), octanol-water partition coefficients (log Kow), acid dissociation constants (pKa), quantification, and identification ions (m/z) of target benzotriazole UV stabilizers; Figure S1: chromatogram of the studied benzotriazole UV stabilizers; Figure S2: mass spectra recorded during GC-MS analysis of studied compounds; Figure S3: comparison of the UV stabilizers peak areas depending on the different extractants; Figure S4: calibration curves used to calculate temporary benzotriazole concentrations; Table S2: experimental and predicted removal efficiency values, for benzotriazole UV stabilizers degradation in the Fe^{2+}/PAA process; Table S3: experimental and predicted removal efficiency for benzotriazole UV stabilizers degradation in the Co^{2+}/PAA process; Table S4: ANOVA results for the UV-P removal process in the Fe^{2+}/PAA system; Table S5: ANOVA results for the UV-326 removal process in the Fe^{2+}/PAA system; Table S6: ANOVA results for the UV-327 removal process in the Fe^{2+}/PAA system; Table S7: ANOVA results for the UV-328 removal process in the Fe^{2+}/PAA system; Table S8: ANOVA results for the UV-329 removal process in the Fe^{2+}/PAA system; Table S9: ANOVA results for the UV-P removal process in the Co^{2+}/PAA system; Table S10: ANOVA results for the UV-329 removal pro-

cess in the Co^{2+}/PAA system; Figure S5: Pareto charts showing the influence of factors and their interactions on the individual BUVs's removal efficiency in the Fe^{2+}/PAA process; Figure S6: Pareto charts showing the influence of factors and their interactions on the individual BUVs's removal efficiency in the Co^{2+}/PAA process; Figure S7: response surface plots of the removal efficiency of studied BUVs in the Fe^{2+}/PAA process; Figure S8: response surface plots of the removal efficiency of studied BUVs in the Co^{2+}/PAA process; Figure S9: mass spectra of post-reaction mixture; Table S11: proposed structures of benzotriazole UV stabilizers oxidation products. Reference [82] is cited in the supplementary materials.

Author Contributions: Conceptualization, U.K. and J.K.; methodology, U.K.; software, D.K.; validation, U.K. and D.K.; investigation, D.K.; data curation, D.K.; writing—original draft preparation, D.K.; writing—review and editing, D.K., U.K. and J.K.; visualization, D.K.; supervision, U.K.; project administration, D.K., U.K. and J.K.; funding acquisition, U.K. and J.K. All authors have read and agreed to the published version of the manuscript.

Funding: This work was funded by the National Science Centre Poland, grant no. 2019/33/B/NZ8/00012, and by the "Innovation Incubator 4.0" program of the Polish Ministry of Science and Higher Education, co-financed by the European Union under the European Regional Development Fund.

Institutional Review Board Statement: Not applicable.

Informed Consent Statement: Not applicable.

Data Availability Statement: Not applicable.

Acknowledgments: We would like to express our gratitude to Margaret Leigh Avera for the linguistic revision of this work and to Michał Sienkiewicz, from the Department of Organic Chemistry, University of Bialystok, for carrying out the ESI-MS analysis.

Conflicts of Interest: The authors declare no conflict of interest. The funders had no role in the design of the study; in the collection, analyses, or interpretation of data; in the writing of the manuscript; or in the decision to publish the results.

References

1. UV Absorbers Market Global Forecast to 2022 | MarketsandMarkets. Available online: https://www.marketsandmarkets.com/Market-Reports/uv-absorber-market-39452163.html (accessed on 26 February 2022).
2. UV Stabilizers. In *Handbook of UV Degradation and Stabilization*; Elsevier: Amsterdam, The Netherlands, 2015; pp. 67–139.
3. Heller, H.; Keller, E.; Land, B.; Gysling, H.; Basel, N.; Mindermann, F. United States Patent Office Ultraviolet Light Absorbed Composition of Matter. US3004896A, 17 October 1961.
4. Cantwell, M.G.; Sullivan, J.C.; Burgess, R.M. Benzotriazoles: History, Environmental Distribution, and Potential Ecological Effects. In *Comprehensive Analytical Chemistry*; Elsevier: Amsterdam, The Netherlands, 2015; Volume 67, pp. 513–545.
5. Smyrniotakis, C.G.; Archontaki, H.A. Development and Validation of a Non-Aqueous Reversed-Phase High-Performance Liquid Chromatographic Method for the Determination of Four Chemical UV Filters in Suncare Formulations. *J. Chromatogr. A* **2004**, *1031*, 319–324. [CrossRef] [PubMed]
6. Wang, X.; Wang, J.; Du, T.; Kou, H.; Du, X.; Lu, X. Determination of Six Benzotriazole Ultraviolet Filters in Water and Cosmetic Samples by Graphene Sponge-Based Solid-Phase Extraction Followed by High-Performance Liquid Chromatography. *Anal. Bioanal. Chem.* **2018**, *410*, 6955–6962. [CrossRef] [PubMed]
7. OECD Existing Chemicals Database. Available online: http://webnet.oecd.org/hpv/ui/Search.aspx (accessed on 7 July 2021).
8. SPIN Substances in Preparations in Nordic Countries. Available online: http://spin2000.net/ (accessed on 7 July 2021).
9. Parajulee, A.; Lei, Y.D.; Kananathalingam, A.; Mitchell, C.P.J.; Wania, F. Investigating the Sources and Transport of Benzotriazole UV Stabilizers during Rainfall and Snowmelt across an Urbanization Gradient. *Environ. Sci. Technol.* **2018**, *52*, 2595–2602. [CrossRef] [PubMed]
10. Zhao, X.; Zhang, Z.F.; Xu, L.; Liu, L.Y.; Song, W.W.; Zhu, F.J.; Li, Y.F.; Ma, W.L. Occurrence and Fate of Benzotriazoles UV Filters in a Typical Residential Wastewater Treatment Plant in Harbin, China. *Environ. Pollut.* **2017**, *227*, 215–222. [CrossRef]
11. Ruan, T.; Liu, R.; Fu, Q.; Wang, T.; Wang, Y.; Song, S.; Wang, P.; Teng, M.; Jiang, G. Concentrations and Composition Profiles of Benzotriazole UV Stabilizers in Municipal Sewage Sludge in China. *Environ. Sci. Technol.* **2012**, *46*, 2071–2079. [CrossRef] [PubMed]
12. Montesdeoca-Esponda, S.; Álvarez-Raya, C.; Torres-Padrón, M.E.; Sosa-Ferrera, Z.; Santana-Rodríguez, J.J. Monitoring and Environmental Risk Assessment of Benzotriazole UV Stabilizers in the Sewage and Coastal Environment of Gran Canaria (Canary Islands, Spain). *J. Environ. Manag.* **2019**, *233*, 567–575. [CrossRef]
13. Casado, J.; Rodríguez, I.; Carpinteiro, I.; Ramil, M.; Cela, R. Gas Chromatography Quadrupole Time-of-Flight Mass Spectrometry Determination of Benzotriazole Ultraviolet Stabilizers in Sludge Samples. *J. Chromatogr. A* **2013**, *1293*, 126–132. [CrossRef]

14. Zhang, Z.; Ren, N.; Li, Y.F.; Kunisue, T.; Gao, D.; Kannan, K. Determination of Benzotriazole and Benzophenone UV Filters in Sediment and Sewage Sludge. *Environ. Sci. Technol.* **2011**, *45*, 3909–3916. [CrossRef]
15. Kotowska, U.; Struk-Sokołowska, J.; Piekutin, J. Simultaneous Determination of Low Molecule Benzotriazoles and Benzotriazole UV Stabilizers in Wastewater by Ultrasound-Assisted Emulsification Microextraction Followed by GC–MS Detection. *Sci. Rep.* **2021**, *11*, 10098. [CrossRef]
16. Liu, R.; Ruan, T.; Wang, T.; Song, S.; Guo, F.; Jiang, G. Determination of Nine Benzotriazole UV Stabilizers in Environmental Water Samples by Automated On-Line Solid Phase Extraction Coupled with High-Performance Liquid Chromatography-Tandem Mass Spectrometry. *Talanta* **2014**, *120*, 158–166. [CrossRef]
17. Nakata, H.; Murata, S.; Filatreau, J. Occurrence and Concentrations of Benzotriazole UV Stabilizers in Marine Organisms and Sediments from the Ariake Sea, Japan. *Environ. Sci. Technol.* **2009**, *43*, 6920–6926. [CrossRef] [PubMed]
18. Nakata, H.; Shinohara, R.I.; Murata, S.; Watanabe, M. Detection of Benzotriazole UV Stabilizers in the Blubber of Marine Mammals by Gas Chromatography-High Resolution Mass Spectrometry (GC-HRMS). *J. Environ. Monit.* **2010**, *12*, 2088–2092. [CrossRef] [PubMed]
19. Apel, C.; Tang, J.; Ebinghaus, R. Environmental Occurrence and Distribution of Organic UV Stabilizers and UV Filters in the Sediment of Chinese Bohai and Yellow Seas. *Environ. Pollut.* **2018**, *235*, 85–94. [CrossRef] [PubMed]
20. Wick, A.; Jacobs, B.; Kunkel, U.; Heininger, P.; Ternes, T.A. Benzotriazole UV Stabilizers in Sediments, Suspended Particulate Matter and Fish of German Rivers: New Insights into Occurrence, Time Trends and Persistency. *Environ. Pollut.* **2016**, *212*, 401–412. [CrossRef]
21. Vimalkumar, K.; Arun, E.; Krishna-Kumar, S.; Poopal, R.K.; Nikhil, N.P.; Subramanian, A.; Babu-Rajendran, R. Occurrence of Triclocarban and Benzotriazole Ultraviolet Stabilizers in Water, Sediment, and Fish from Indian Rivers. *Sci. Total Environ.* **2018**, *625*, 1351–1360. [CrossRef]
22. Lu, Z.; De Silva, A.O.; Zhou, W.; Tetreault, G.R.; de Solla, S.R.; Fair, P.A.; Houde, M.; Bossart, G.; Muir, D.C.G. Substituted Diphenylamine Antioxidants and Benzotriazole UV Stabilizers in Blood Plasma of Fish, Turtles, Birds and Dolphins from North America. *Sci. Total Environ.* **2019**, *647*, 182–190. [CrossRef]
23. Lu, Z.; De Silva, A.O.; Peart, T.E.; Cook, C.J.; Tetreault, G.R.; Servos, M.R.; Muir, D.C.G. Distribution, Partitioning and Bioaccumulation of Substituted Diphenylamine Antioxidants and Benzotriazole UV Stabilizers in an Urban Creek in Canada. *Environ. Sci. Technol.* **2016**, *17*, 9089–9097. [CrossRef]
24. Kim, J.W.; Isobe, T.; Malarvannan, G.; Sudaryanto, A.; Chang, K.H.; Prudente, M.; Tanabe, S. Contamination of Benzotriazole Ultraviolet Stabilizers in House Dust from the Philippines: Implications on Human Exposure. *Sci. Total Environ.* **2012**, *424*, 174–181. [CrossRef]
25. Carpinteiro, I.; Abuín, B.; Rodríguez, I.; Ramil, M.; Cela, R. Pressurized Solvent Extraction Followed by Gas Chromatography Tandem Mass Spectrometry for the Determination of Benzotriazole Light Stabilizers in Indoor Dust. *J. Chromatogr. A* **2010**, *1217*, 3729–3735. [CrossRef]
26. Maceira, A.; Borrull, F.; Marcé, R.M. Occurrence of Plastic Additives in Outdoor Air Particulate Matters from Two Industrial Parks of Tarragona, Spain: Human Inhalation Intake Risk Assessment. *J. Hazard. Mater.* **2019**, *373*, 649–659. [CrossRef]
27. Montesdeoca-Esponda, S.; Torres-Padrón, M.E.; Sosa-Ferrera, Z.; Santana-Rodríguez, J.J. Fate and Distribution of Benzotriazole UV Filters and Stabilizers in Environmental Compartments from Gran Canaria Island (Spain): A Comparison Study. *Sci. Total Environ.* **2021**, *756*, 144086. [CrossRef] [PubMed]
28. Gimeno-Monforte, S.; Montesdeoca-Esponda, S.; Sosa-Ferrera, Z.; Santana-Rodríguez, J.J.; Castro, Ó.; Pocurull, E.; Borrull, F. Multiresidue Analysis of Organic UV Filters and UV Stabilizers in Fish of Common Consumption. *Foods* **2020**, *9*, 1827. [CrossRef] [PubMed]
29. Kim, J.-W.; Ramaswamy, R.; Chang, K.-H.; Isobe, T.; Tanabe, S. Multiresidue Analytical Method for the Determination of Antimicrobials, Preservatives, Benzotriazole UV Stabilizers, Flame Retardants and Plasticizers in Fish Using Ultra High Performance Liquid Chromatography Coupled with Tandem Mass Spectrometry. *J. Chromatogr. A* **2011**, *1218*, 3511–3520. [CrossRef] [PubMed]
30. Lu, Z.; De Silva, A.O.; Peart, T.E.; Cook, C.J.; Tetreault, G.R. Tissue Distribution of Substituted Diphenylamine Antioxidants and Benzotriazole Ultraviolet Stabilizers in White Sucker (Catostomus Commersonii) from an Urban Creek in Canada. *Environ. Sci. Technol. Lett.* **2017**, *4*, 433–438. [CrossRef]
31. Zhu, M.Q.; Cui, R. Determination of UV-327 and UV-328 in Mouse Plasma by High Performance Liquid Chromatography. *Beijing Da Xue Xue Bao.* **2020**, *52*, 591–596. [CrossRef] [PubMed]
32. Lee, S.; Kim, S.; Park, J.; Kim, H.J.; Jae Lee, J.; Choi, G.; Choi, S.; Kim, S.; Young Kim, S.; Choi, K.; et al. Synthetic Musk Compounds and Benzotriazole Ultraviolet Stabilizers in Breast Milk: Occurrence, Time-Course Variation and Infant Health Risk. *Environ. Res.* **2015**, *140*, 466–473. [CrossRef]
33. Kim, J.W.; Chang, K.H.; Prudente, M.; Viet, P.H.; Takahashi, S.; Tanabe, S.; Kunisue, T.; Isobe, T. Occurrence of Benzotriazole Ultraviolet Stabilizers (BUVSs) in Human Breast Milk from Three Asian Countries. *Sci. Total Environ.* **2019**, *655*, 1081–1088. [CrossRef]
34. Molins-Delgado, D.; Olmo-Campos, M.d.M.; Valeta-Juan, G.; Valeta-Juan, G.; Pleguezuelos-Hernández, V.; Barceló, D.; Díaz-Cruz, M.S. Determination of UV Filters in Human Breast Milk Using Turbulent Flow Chromatography and Babies' Daily Intake Estimation. *Environ. Res.* **2018**, *161*, 532–539. [CrossRef]

35. Environment and Climate Change Canada; Health Canada. *Draft Screening Assessment Benzotriazoles and Benzothiazoles Group*; Government of Canada: Ottawa, ON, Canada, 2021.
36. Nakata, H.; Shinohara, R.I.; Nakazawa, Y.; Isobe, T.; Sudaryanto, A.; Subramanian, A.; Tanabe, S.; Zakaria, M.P.; Zheng, G.J.; Lam, P.K.S.; et al. Asia-Pacific Mussel Watch for Emerging Pollutants: Distribution of Synthetic Musks and Benzotriazole UV Stabilizers in Asian and US Coastal Waters. *Mar. Pollut. Bull.* **2012**, *64*, 2211–2218. [CrossRef]
37. Nagayoshi, H.; Kakimoto, K.; Takagi, S.; Konishi, Y.; Kajimura, K.; Matsuda, T. Benzotriazole Ultraviolet Stabilizers Show Potent Activities as Human Aryl Hydrocarbon Receptor Ligands. *Environ. Sci. Technol.* **2015**, *49*, 578–587. [CrossRef]
38. Geneva International Conference Centre (CICG). Ninth Meeting of the Conference of the Parties to the Stockholm Convention. In Proceedings of the Stockholm Convention of Persistent Organic Pollutants Report of the Conference of the Parties to the Stockholm Convention on Persistent Organic Pollutants on the Work of Its Ninth Meeting, Geneva, Switzerland, 29 April–10 May 2019.
39. Fent, K.; Chew, G.; Li, J.; Gomez, E. Benzotriazole UV-Stabilizers and Benzotriazole: Antiandrogenic Activity in Vitro and Activation of Aryl Hydrocarbon Receptor Pathway in Zebrafish Eleuthero-Embryos. *Sci. Total Environ.* **2014**, *482–483*, 125–136. [CrossRef] [PubMed]
40. Feng, H.; Cao, H.; Li, J.; Zhang, H.; Xue, Q.; Liu, X.; Zhang, A.; Fu, J. Estrogenic Activity of Benzotriazole UV Stabilizers Evaluated through in Vitro Assays and Computational Studies. *Sci. Total Environ.* **2020**, *727*, 138549. [CrossRef] [PubMed]
41. Fischer, C.; Leibold, E.; Göen, T. Identification of in Vitro Phase I Metabolites of Benzotriazole UV Stabilizer UV-327 Using HPLC Coupled with Mass Spectrometry. *Toxicol. Vitr.* **2020**, *68*, 104932. [CrossRef]
42. Denghel, H.; Leibold, E.; Göen, T. Oxidative Phase I Metabolism of the UV Absorber 2-(2H-Benzotriazol-2-Yl)-4,6-Di-Tert-Pentylphenol (UV 328) in an in Vitro Model with Human Liver Microsomes. *Toxicol. Vitr.* **2019**, *60*, 313–322. [CrossRef]
43. Denghel, H.; Göen, T. Determination of the UV Absorber 2-(2H-Benzotriazol-2-Yl)-4,6-Di-Tert-Pentylphenol (UV 328) and Its Oxidative Metabolites in Human Urine by Dispersive Liquid-Liquid Microextraction and GC–MS/MS. *J. Chromatogr. B Anal. Technol. Biomed. Life Sci.* **2020**, *1144*, 122071. [CrossRef]
44. Denghel, H.; Göen, T. Dispersive Liquid-Liquid Microextraction (DLLME) and External Real Matrix Calibration for the Determination of the UV Absorber 2-(2H-Benzotriazol-2-Yl)-4,6-Di-Tert-Pentylphenol (UV 328) and Its Metabolites in Human Blood. *Talanta* **2021**, *223*, 121699. [CrossRef]
45. Zhuang, S.; Lv, X.; Pan, L.; Lu, L.; Ge, Z.; Wang, J.; Wang, J.; Liu, J.; Liu, W.; Zhang, C. Benzotriazole UV 328 and UV-P Showed Distinct Antiandrogenic Activity upon Human CYP3A4-Mediated Biotransformation. *Environ. Pollut.* **2017**, *220*, 616–624. [CrossRef]
46. Liang, X.; Li, J.; Martyniuk, C.J.; Wang, J.; Mao, Y.; Lu, H.; Zha, J. Benzotriazole Ultraviolet Stabilizers Alter the Expression of the Thyroid Hormone Pathway in Zebrafish (Danio Rerio) Embryos. *Chemosphere* **2017**, *182*, 22–30. [CrossRef]
47. Hemalatha, D.; Rangasamy, B.; Nataraj, B.; Maharajan, K.; Narayanasamy, A.; Ramesh, M. Transcriptional, Biochemical and Histological Alterations in Adult Zebrafish (Danio Rerio) Exposed to Benzotriazole Ultraviolet Stabilizer-328. *Sci. Total Environ.* **2020**, *739*, 139851. [CrossRef]
48. Giraudo, M.; Cottin, G.; Esperanza, M.; Gagnon, P.; Silva, A.O.D.; Houde, M. Transcriptional and Cellular Effects of Benzotriazole UV Stabilizers UV-234 and UV-328 in the Freshwater Invertebrates Chlamydomonas Reinhardtii and Daphnia Magna. *Environ. Toxicol. Chem.* **2017**, *36*, 3333–3342. [CrossRef] [PubMed]
49. Kim, J.W.; Chang, K.H.; Isobe, T.; Tanabe, S. Acute Toxicity of Benzotriazole Ultraviolet Stabilizers on Freshwater Crustacean (Daphnia Pulex). *J. Toxicol. Sci.* **2011**, *36*, 247–251. [CrossRef] [PubMed]
50. Lee, J.K.; Kim, K.B.; Lee, J.D.; Shin, C.Y.; Kwack, S.J.; Lee, B.M.; Lee, J.Y. Risk Assessment of Drometrizole, a Cosmetic Ingredient Used as an Ultraviolet Light Absorber. *Toxicol. Res.* **2019**, *35*, 119–129. [CrossRef] [PubMed]
51. 2-(2H-Benzotriazol-2-Yl)-4,6-Ditertpentylphenol—Brief Profile—ECHA. Available online: https://www.echa.europa.eu/de/web/guest/brief-profile/-/briefprofile/100.043.062 (accessed on 8 July 2021).
52. Annex XV-Identification of UV-328 as SVHC Annex XV Dossier. Available online: https://echa.europa.eu/documents/10162/13641/rac_opinion_annex_UV-328_en.pdf/6d264702-380f-45d4-8022-fb59ca44740f (accessed on 8 July 2021).
53. Luukkonen, T.; Teeriniemi, J.; Prokkola, H.; Rämö, J.; Lassi, U. Chemical Aspects of Peracetic Acid Based Wastewater Disinfection. *Water SA* **2014**, *40*, 73–80. [CrossRef]
54. Kiejza, D.; Kotowska, U.; Polińska, W.; Karpińska, J. Peracids - New Oxidants in Advanced Oxidation Processes: The Use of Peracetic Acid, Peroxymonosulfate, and Persulfate Salts in the Removal of Organic Micropollutants of Emerging Concern—A Review. *Sci. Total Environ.* **2021**, *790*, 148195. [CrossRef]
55. Ao, X.-w.; Eloranta, J.; Huang, C.H.; Santoro, D.; Sun, W.-j.; Lu, Z.-d.; Li, C. Peracetic Acid-Based Advanced Oxidation Processes for Decontamination and Disinfection of Water: A Review. *Water Res.* **2021**, *188*, 116479. [CrossRef]
56. Kim, J.; Huang, C.-H. Reactivity of Peracetic Acid with Organic Compounds: A Critical Review. *ACS ES&T Water* **2021**, *1*, 15–33. [CrossRef]
57. Cai, M.; Sun, P.; Zhang, L.; Huang, C.H. UV/Peracetic Acid for Degradation of Pharmaceuticals and Reactive Species Evaluation. *Environ. Sci. Technol.* **2017**, *51*, 14217–14224. [CrossRef]
58. Hollman, J.; Dominic, J.A.; Achari, G. Degradation of Pharmaceutical Mixtures in Aqueous Solutions Using UV/Peracetic Acid Process: Kinetics, Degradation Pathways and Comparison with UV/H2O2. *Chemosphere* **2020**, *248*, 125911. [CrossRef]
59. Zhang, L.; Liu, Y.; Fu, Y. Degradation Kinetics and Mechanism of Diclofenac by UV/Peracetic Acid. *RSC Adv.* **2020**, *10*, 9907–9916. [CrossRef]

60. Rizzo, L.; Agovino, T.; Nahim-Granados, S.; Castro-Alférez, M.; Fernández-Ibáñez, P.; Polo-López, M.I. Tertiary Treatment of Urban Wastewater by Solar and UV-C Driven Advanced Oxidation with Peracetic Acid: Effect on Contaminants of Emerging Concern and Antibiotic Resistance. *Water Res.* **2019**, *149*, 272–281. [CrossRef] [PubMed]
61. Kim, J.; Du, P.; Liu, W.; Luo, C.; Zhao, H.; Huang, C.H. Cobalt/Peracetic Acid: Advanced Oxidation of Aromatic Organic Compounds by Acetylperoxyl Radicals. *Environ. Sci. Technol.* **2020**, *54*, 5268–5278. [CrossRef] [PubMed]
62. Wang, Z.; Wang, J.; Xiong, B.; Bai, F.; Wang, S.; Wan, Y.; Zhang, L.; Xie, P.; Wiesner, M.R. Application of Cobalt/Peracetic Acid to Degrade Sulfamethoxazole at Neutral Condition: Efficiency and Mechanisms. *Environ. Sci. Technol.* **2019**, *54*, 464–475. [CrossRef]
63. Popov, E.; Eloranta, J.; Hietapelto, V.; Vuorenpalo, V.M.; Aksela, R.; Jäkärä, J. Mechanism of Decomposition of Peracetic Acid by Manganese Ions and Diethylenetriaminepentaacetic Acid (DTPA). *Holzforschung* **2005**, *59*, 507–513. [CrossRef]
64. Zhang, X.-Z.; Francis, R.C.; Dutton, D.B.; Hill, R.T. Decomposition of Peracetic Acid Catalyzed by Cobalt(II) and Vanadium(V). *Can. J. Chem.* **1998**, *76*, 1064–1069. [CrossRef]
65. Zhou, F.; Lu, C.; Yao, Y.; Sun, L.; Gong, F.; Li, D.; Pei, K.; Lu, W.; Chen, W. Activated Carbon Fibers as an Effective Metal-Free Catalyst for Peracetic Acid Activation: Implications for the Removal of Organic Pollutants. *Chem. Eng. J.* **2015**, *281*, 953–960. [CrossRef]
66. Wu, W.; Tian, D.; Liu, T.; Chen, J.; Huang, T.; Zhou, X.; Zhang, Y. Degradation of Organic Compounds by Peracetic Acid Activated with Co3O4: A Novel Advanced Oxidation Process and Organic Radical Contribution. *Chem. Eng. J.* **2020**, *394*, 124938. [CrossRef]
67. Rokhina, E.V.; Makarova, K.; Lahtinen, M.; Golovina, E.A.; Van As, H.; Virkutyte, J. Ultrasound-Assisted MnO2 Catalyzed Homolysis of Peracetic Acid for Phenol Degradation: The Assessment of Process Chemistry and Kinetics. *Chem. Eng. J.* **2013**, *221*, 476–486. [CrossRef]
68. Wang, J.; Xiong, B.; Miao, L.; Wang, S.; Xie, P.; Wang, Z.; Ma, J. Applying a Novel Advanced Oxidation Process of Activated Peracetic Acid by CoFe2O4 to Efficiently Degrade Sulfamethoxazole. *Appl. Catal. B Environ.* **2021**, *280*, 119422. [CrossRef]
69. Wang, J.; Wang, Z.; Cheng, Y.; Cao, L.; Bai, F.; Yue, S.; Xie, P.; Ma, J. Molybdenum Disulfide (MoS2): A Novel Activator of Peracetic Acid for the Degradation of Sulfonamide Antibiotics. *Water Res.* **2021**, *201*, 117291. [CrossRef]
70. Zhou, X.; Hao, W.; Zhang, L.; Liang, B.; Sun, X.; Chen, J. Activation of Peracetic Acid with Lanthanum Cobaltite Perovskite for Sulfamethoxazole Degradation under a Neutral PH: The Contribution of Organic Radicals. *Molecules* **2020**, *25*, 2725. [CrossRef] [PubMed]
71. Wang, S.; Wang, H.; Liu, Y.; Fu, Y. Effective Degradation of Sulfamethoxazole with Fe^{2+}-Zeolite/Peracetic Acid. *Sep. Purif. Technol.* **2020**, *233*, 115973. [CrossRef]
72. Liu, Y.S.; Ying, G.G.; Shareef, A.; Kookana, R.S. Occurrence and Removal of Benzotriazoles and Ultraviolet Filters in a Municipal Wastewater Treatment Plant. *Environ. Pollut.* **2012**, *165*, 225–232. [CrossRef] [PubMed]
73. Chen, X.; Wang, J.; Chen, J.; Zhou, C.; Cui, F.; Sun, G. Photodegradation of 2-(2-Hydroxy-5-Methylphenyl)Benzotriazole (UV-P) in Coastal Seawaters: Important Role of DOM. *J. Environ. Sci. (China)* **2019**, *85*, 129–137. [CrossRef]
74. Pavanello, A.; Gomez-Mendoza, M.; de la Peña O'Shea, V.A.; Miranda, M.A.; Marin, M.L. Degradation of Benzotriazole UV-Stabilizers in the Presence of Organic Photosensitizers and Visible Light: A Time-Resolved Mechanistic Study. *J. Photochem. Photobiol. B Biol.* **2022**, *230*, 112444. [CrossRef]
75. Kim, J.; Zhang, T.; Liu, W.; Du, P.; Dobson, J.T.; Huang, C.H. Advanced Oxidation Process with Peracetic Acid and Fe(II) for Contaminant Degradation. *Environ. Sci. Technol.* **2019**, *53*, 13312–13322. [CrossRef]
76. El-Asmy, H.A.; Butler, I.S.; Mouhri, Z.S.; Jean-Claude, B.J.; Emmam, M.S.; Mostafa, S.I. Zinc(II), Ruthenium(II), Rhodium(III), Palladium(II), Silver(I), Platinum(II) and MoO_2^{2+} Complexes of 2-(2′-Hydroxy-5′-Methylphenyl)-Benzotriazole as Simple or Primary Ligand and 2,2′-Bipyridyl, 9,10-Phenanthroline or Triphenylphosphine as Secondary Ligands: Structure and Anticancer Activity. *J. Mol. Struct.* **2014**, *1059*, 193–201. [CrossRef]
77. Alfassi, Z.B.; Schuler, R.H. Reaction of Azide Radicals with Aromatic Compounds. Azide as a Selective Oxidant. *J. Phys. Chem.* **1985**, *89*, 3359–3363. [CrossRef]
78. McKeown, E.; Waters, W.A. The Oxidation of Organic Compounds by "Singlet" Oxygen. *J. Chem. Soc. B Phys. Org.* **1966**, 1040–1046. [CrossRef]
79. Lai, H.J.; Ying, G.G.; Ma, Y.B.; Chen, Z.F.; Chen, F.; Liu, Y.S. Occurrence and Dissipation of Benzotriazoles and Benzotriazole Ultraviolet Stabilizers in Biosolid-Amended Soils. *Environ. Toxicol. Chem.* **2014**, *33*, 761–767. [CrossRef]
80. Brandt, M.; Becker, E.; Jöhncke, U.; Sättler, D.; Schulte, C. A Weight-of-Evidence Approach to Assess Chemicals: Case Study on the Assessment of Persistence of 4,6-Substituted Phenolic Benzotriazoles in the Environment. *Environ. Sci. Eur.* **2016**, *28*, 1–14. [CrossRef] [PubMed]
81. Wu, J.; Xiong, Q.; Liang, J.; He, Q.; Yang, D.; Deng, R.; Chen, Y. Degradation of Benzotriazole by DBD Plasma and Peroxymonosulfate: Mechanism, Degradation Pathway and Potential Toxicity. *Chem. Eng. J.* **2020**, *384*, 123300. [CrossRef]
82. Luukkonen, T. *New Adsorption and Oxidation-Based Approaches for Water and Wastewater Treatment*; Studies Regarding Organic Peracids, Boiler-Water Treatment, and Geopolymers, University of Oulu Graduate School; University of Oulu, Faculty of Science: Oulu, Finland, 2016.